Intact carbonic acid is a viable protonating agent for biological bases

Daniel Aminov, Dina Pines, Philip M Kiefer, Snehasis Daschakraborty, James T. Hynes, Ehud Pines

Carbonic acid: A viable protonating agent for biological bases

Daniel Aminov[a], Dina Pines[a], Philip M. Kiefer[b], Snehasis Daschakraborty[b,], James T. Hynes[b,c,1,], and Ehud Pines[a,1]

[a]Department of Chemistry, Ben-Gurion University of the Negev, P.O. Box 653, Beer-Sheva, 84105, Israel;
[b]Department of Chemistry, University of Colorado, Boulder, CO 80309-0215, U.S.A.;
[c]PASTEUR, Départmente de Chimie, Ecole Normale Supérieure, PSL Research University, Sorbonne Universités, UPMC Univ. Paris 06, CNRS, 75005 Paris, France

[1]To whom correspondence should be addressed. Emails: chynes43@gmail.com, epines@bgu.ac.il

Classification: Physical Sciences, Chemistry

Abstract. Carbonic acid H_2CO_3 (CA) is a key constituent of the universal CA/bicarbonate/CO_2 buffer maintaining the pH of both blood and the oceans. Here we demonstrate the ability of intact CA to quantitatively protonate bases with biologically-relevant pK_a's and argue that CA has a previously unappreciated function as a major source of protons in blood-plasma. We determine with high precision the temperature dependence of pK_a(CA), $pK_a(T) = -373.604 + 16500/T+56.478\ln T$. At physiological-like conditions pK_a(CA) = 3.45 (I = 0.15M, 37^{o}C), making CA stronger than lactic acid. We further demonstrate experimentally that CA decomposition to H_2O and CO_2 does not impair its ability to act as an ordinary carboxylic acid and to efficiently protonate physiological-like bases. The consequences of this conclusion are far reaching for human physiology and marine biology. While CA is somewhat less reactive than $(H^+)_{aq}$, it is more than one order of magnitude more abundant than $(H^+)_{aq}$ in the blood plasma and in the oceans. In particular, CA is about 70 times more abundant than $(H^+)_{aq}$ in the blood plasma, where we argue that its overall protonation efficiency is 10-20 times greater than $(H^+)_{aq}$, often considered to be the major protonating agent there. CA should thus function as a major source for fast in-vivo acid-base reactivity in the blood plasma possibly penetrating intact into membranes and significantly helping to compensate for $(H^+)_{aq}$'s kinetic deficiency in sustaining the large proton fluxes that are vital for metabolic processes and rapid enzymatic reactions.

Keywords: carbonic acid, protonation of biological bases, biological buffers

Significance statement. The MS demonstrates the previously unappreciated feature that, despite its instability, carbonic acid (CA) acts as an effective protonating agent consistent with its pK_a value, which is here accurately determined over the full physiological temperature range. The equilibrium concentration of CA in the blood plasma is about 70 times larger than $(H^+)_{aq}$, and, given CA's acidic reactivity established here, it is concluded that, in contrast to current thought, CA should be considered a far more important protonation agent in the blood than is $(H^+)_{aq}$,. These novel conclusions should be also considered when evaluating conditions resulting in CA concentration increase, such as acidosis in the physiological context and the gradual acidification of the oceans in the environmental setting.

\body The idea of biological reactivity driven and regulated by enzymes and specific reactions of designed biological molecules has played a major role in biochemistry's development (1,2). But

this perspective can overshadow important aspects of biochemical processes driven non-specifically in the physiological environment such as reactions driven by a concentration gradient. A particular instance is the protonation reactions of bases or basic groups driven by largely homogeneous populations of either aqueous protons $(H^+)_{aq}$ (3,4) or mobile acids such as those participating in the physiological buffer system (5,6) Here we argue – based on experimental observations described within – that a key role in this connection is played by a previously unappreciated major proton source: carbonic acid (CA) H_2CO_3. In particular, we focus on the protonation of bio-relevant bases B by CA

$$B + H_2CO_3 \underset{k_{off}}{\overset{k_{on}}{\rightleftarrows}} H^+B + HCO_3^- \qquad (1)$$

where HCO_3^- is the bicarbonate anion. (the rate constants here will be discussed within). While it deals with experiments on CA in aqueous solution, this paper focusses on the issue of the significance of CA in the blood plasma.

CA is an invariable constituent of the universal H_2CO_3 / HCO_3^- / CO_2 buffer ('the CA buffer') which helps maintain the pH of both the blood plasma (7-9) and the earth's seas and oceans(10-15). The CA buffer constitutes about 83% of blood plasma's buffer capacity and about 53% of the whole blood capacity (16,17) and, as the blood's 'front-line' buffer, is extremely important for human physiology (7,8). It is regulated in the body by one of nature's most efficient enzymes, Carbonic Anhydrase (18,19). It is crucial that the very large HCO_3^- concentration (26-28 mM) (1,2,7-9) in equilibrium with CA makes CA a permanent factor in the plasma, with an equilibrium 2-3 μM concentration, about 70 times larger than $[H^+]_{aq}$. Finally, the CA buffer is a critical respiratory system component, responsible for CO_2 transport across membranes (5, 6, 9, 20,21).
CA's chemistry is dominated by its spontaneous breakdown (22) in bulk water into CO_2 and H_2O

$$H_2CO_3 \underset{k_{CA}}{\overset{k_{dc}}{\rightleftarrows}} H_2O + CO_2 \qquad (2)$$

with a first-order decomposition reaction rate constant k_{dc} (corresponding to a decomposition lifetime $\tau_{dc} = 1/k_{dc}$ of about 60 ms (20°C)), which is about 300 times larger than the pseudo first order back-hydration rate constant k_{CA} (23-28). CA decomposes via a proton chain mechanism in aqueous solution – and even in the gas-phase in the presence of a single water molecule (29-34).

The reverse reaction in equation (2) – CO_2 reacting with water to form H_2CO_3 – is bimolecular, dependent on the CO_2 concentration, and is the cause of CA's small equilibrium concentration in aqueous solution). CA's aqueous solutions are slightly acidic through the CA reversible proton dissociation reaction

$$H_2CO_3 \underset{k_{D(BC)}}{\overset{k_{dis(CA)}}{\rightleftarrows}} (H^+)_{aq} + HCO_3^- \quad (3)$$

Here $k_{dis(CA)}$ is CA's overall acid dissociation rate constant and $k_{D(BC)}$ is the diffusion-limited rate constant of the back protonation of HCO_3^- to reform CA (23-26). In physiological systems, $k_{dis(CA)}$ and $k_{D(BC)}$ depend on the particular environment, with CA's equilibrium constant $K_a(CA) = k_{dis(CA)}/ k_{D(BC)}$. (In the blood, the Carbonic Anhydrase enzyme likely accelerates regeneration of CA (18,19), otherwise regenerated via uncatalyzed reaction (2) and protonation of HCO_3^- equation (3)). The enzyme Carbonic Anhydrase just mentioned catalyzes equation (2) reactions with very high turnover of 10^4 to 10^6 CO_2 molecules/second (21). It thereby helps regulate the blood plasma's pH and CA levels, and – with the very large HCO_3^- concentration (26-28 mM)

(1,2,7-9) in equilibrium with CA – makes the CA concentration an undiminished permanent factor in the blood plasma with a 2-3 μM equilibrium concentration.

In the context of human physiology, the importance of resolving the physiological role of CA stems from this relatively-high steady-state concentration of CA, which is about 70 times larger that that of $(H^+)_{aq}$ (7,8), its potential considerable reactivity as a moderately strong carboxylic acid, and from the physiological demand for fast in-vivo acid-base reactivity. In particular, this demand is absolutely vital to sustain life processes, but it appears to be inconsistent both with the hydrated proton's diminished concentration, $[(H^+)_{aq}] = 40$ nM in the blood plasma (7,8), and with $(H^+)_{aq}$'s reduced diffusivity in biological environments due to impairment of the Grotthuss proton transport mechanism by various hydrophobic entities (35).

In order to demonstrate that CA's presence significantly eases this problem, we must first determine whether CA's instability fatally compromises – as traditionally thought – its chemical reactivity as a sufficiently strong acid of considerable protonation ability. We will argue within that CA's acid-base reactivity equation (1) is not so compromised. The main question here is whether CA is capable of protonating bases by one or both of the standard carboxylic acid – protonation mechanistic routes (discussed within) (36-39), or instead decomposes to H_2O and CO_2, either via equation (2) (23-26) or via a base-catalyzed variant

$$B + H_2CO_3 \underset{k_{CA}}{\overset{k_{ic}}{\rightleftarrows}} B + CO_2 + H_2O \qquad (4)$$

in which maximum value of k_{ic} is reached when the reaction is assumed to be diffusion-controlled, $k_{ic} = k_{D(B)}$ (36-39). Returning to equation (1), it is essential for the physiological problem's solution that we will address is the determination of how efficiently CA protonates bases – if CA acts like a standard Brønsted acid (40), i.e. via standard protonation routes mentioned above – and if that protonation is sufficiently rapid to supply protons on typical, relevant biological timescales.

In the remainder of the paper, we first establish that CA behaves thermodynamically, vis-à-vis its acid equilibrium constant, like any ordinary carboxylic acid such as acetic and formic acids (40). We then demonstrate and analyze CA's kinetic ability to protonate physiological-like bases, and in particular that this protonation dominates decomposition to H_2O and CO_2. Finally, we analyze the protonation by CA's reaction kinetic mechanisms associated with equation (1) and demonstrate that this must in fact be much more efficient – and hence much more physiologically important – than protonation by $(H^+)_{aq}$. With these results, we offer a solution for the above-mentioned major physiological conundrum of the kinetic 'deficiency' of $(H^+)_{aq}$.

Results and Discussion

CA pK_a temperature dependence. To establish that CA behaves as an ordinary protonating (Brønsted) carboxylic acid in a thermodynamic perspective, we determine its pK_a temperature dependence. The 20°C value pK^0_a of intact CA in equilibrium with its HCO_3^- deprotonated form has been recently determined to be about 3.5 (41, 42) at zero ionic strength I = 0 and – as we now report – is about 3.6 (I=0) at the physiologically important 37°C, cf Fig. 1. The reported data are obtained via temperature-dependent stopped-flow experiments (SI Appendix, sec. S7 and Fig. S4).

This key data provides the acid dissociation's important thermodynamic enthalpy and entropy parameters ΔH and ΔS, related to K_a via (43)

$$\Delta G = -RT\ln K_a, \qquad \frac{d\ln K_a}{dT} = \frac{\Delta H}{RT^2}, \qquad (5)$$

with R the gas constant and T the temperature in K at 1 bar pressure.

The data in Fig. 1 are well fit by

$$pK_a(T) = -373.604 + 16500/T + 56.478 \ln T \quad (6)$$

which allows an excellent estimation of pK_a (CA) in the full physiological range of body temperatures from extreme hypothermia to extreme hyperthermia conditions (about 25^0C to 44^0C) (44-49). Further, equations (5) and (6) provide the CA dissociation reaction's standard enthalpy and entropy change at 25°C as -1.5 kcal/mol and -21.2 cal/mol/K, respectively. All this classes CA as an ordinarily-behaved carboxylic acid such as acetic and formic acids: as do they, CA shows a pK_a minimum about room temperature, in the CA case at 19°C = 3.51± 0.02 and exhibits small enthalpy ΔH^o and large entropy ΔS^o changes upon proton dissociation (44-49). Our measurements give CA's dissociation free energy $\Delta G^o = \Delta H^o - T\Delta S^o$ = -1.5 kcal + 6.3 kcal = 4.8 kcal at T = 298 K (pK_a(CA) = 3.52 ± 0.02 at 25°C); it is noteworthy that ΔG^o (CA) is dominated by the $T\Delta S^o$ contribution, another similarity to the stable carboxylic acids (44-49). In conclusion, in this thermodynamic perspective**,** CA behaves just like an ordinary carboxylic acid.

Well-known empirical thermodynamic-kinetics correlations (41, 42, 50-53) would strongly suggest, given the above thermodynamic results, that CA also behaves kinetically as a standard carboxylic acid. But the experimental kinetic character of CA's base protonation ability is in fact currently unknown, and thus requires to be determined, as we now report.

Testing the kinetic viability of CA as a protonating agent. We now turn to the required experimental test of whether – in accordance with its substantial acidity predicted by its thermodynamic K_a value – CA kinetically protonates bases via equation (1) involving the rate constants k_{on} and k_{off} (SI Appendix, equations S3.1 and S3.2) for overall base protonation by intact CA and the deprotonation of BH^+ by HCO_3^- respectively.

For this purpose, we selected two oxygen bases with structures and pK_as relevant to biological systems: the HPTS base 8-hydroxy-1,3,6-trisulfonate anion, and the 1N4S base 1-naphthol-4-sulfonate anion. The pK^o_as (I = 0) of these two bases' conjugate Brønsted acids (H^+Bs) are 7.95 and 8.2 respectively (54, 55). HPTS and 1N4S have basicity similar to that of many important physiological bases such the amine groups in small peptides, the hydroxyl group in Tyrosine, and the imine group in Histidine, whose conjugate acids' pK^o_as all fall in the range of 8 ± 2 (56). This range makes all these bases' conjugate acidity at least 3 pK_a units weaker than CA's, which indicates (*vide infra*) that their protonation by CA should be fast, approaching the diffusion limit.

Turning to the actual experiments, we have conducted stopped-flow experiments utilizing a two-stage rapid mixing procedure. In the first cell, CA was generated by a rapid quantitative acidification by HCl of a pre-chosen fraction of the bicarbonate anion HCO_3^- concentration**,** generating the bicarbonate/CA buffer solution at the desired composition. Following a variable incubation (waiting) time τ_{inc} during which a CA partial loss occurs via the spontaneous decomposition equation (1), the resulting CA solution was mixed in the second cell with the base solution, allowing CA's protonation. Figure 2 shows the protonated base fraction versus τ_{inc}.

For each base B in Fig. 2, the measured protonated base B^+H concentration decreases with a time constant practically equal to that of the independently measured decomposition lifetime of CA [equation (2)]. Thus, the extent of progress of the bases' protonation yields appears to depend *solely* on the incubation time of CA, which in turn determines the amount of intact CA left at the time of mixing with the base solution. The behavior of the protonated base concentration's reduction with longer incubation time in Fig. 2 directly reflects CA's prior decay via equation (2) unaltered by any further kinetic process. This observation leads to an important conclusion: CA's protonation of the base proceeds without any CA concentration *decomposition* loss beyond that which occurred during the incubation time.

The conclusion just stated also implies that the CA's base protonations' timescale is much shorter than CA's time for decomposition occurring within the mixing time of the stopped flow apparatus of about 1 ms – the central conclusion; thus the protonation reaction occurs practically instantaneously compared to both the decomposition and mixing time-scales. This is confirmed by the full numerical solutions of the rate equations for the kinetic scheme for CA's time development. This scheme accounts for all our report's reactions, and is numerically solved for the aqueous solution concentrations of the key species H_2CO_3, HCO_3^-, H^+ and B; it includes reaction equations (2-4) as well as those for the two CA protonation mechanisms mentioned in the Introduction.

As part of this full kinetic scheme we analyze the overall protonation reaction by CA equation (1) in terms of two standard protonation routes. The first is a direct protonation route R_d, with contact protonation occurring according to (36-39)

$$H_2CO_3 + B \underset{k_S}{\overset{k_{D(B)}}{\rightleftarrows}} [B \cdots H_2CO_3]_a \overset{k_p}{\rightarrow} H^+B + HCO_3^- \qquad (7)$$

which includes diffusive complex formation/ dissociation prior to the protonation step. $k_{D(B)}$ are the reactants' diffusion-limited rate constants and k_S is the diffusion-limited rate constant for separating the products from contact to bulk. k_p is the rate constant for the unimolecular (contact) protonation; we estimate its magnitude from free-energy correlations, see SI Appendix for details (the very slow back-protonation of bicarbonate anion to reform CA is neglected (26)). R_d is the main base protonation route for bimolecular protonation by weak acids, whose acid dissociation rate is not large compared to their bimolecular base-encounter rate.

The standard second pathway is an indirect protonation route R_i, in which the acid first dissociates to produce a hydrated proton $(H^+)_{aq}$, which then protonates the base (36-39)

$$H_2CO_3 + B \underset{k_{D(BC)}}{\overset{k_{dis(CA)}}{\rightleftarrows}} (H^+)_{aq} + B + HCO_3^- \underset{k_{dis(HB)}}{\overset{k_{D(HB)}}{\rightleftarrows}} HCO_3^- + H^+ \quad (8)$$

with $k_{D(BC)}$ and $k_{dis(CA)}$ defined as in equation (3). This route involves the diffusive recombination of ions to reform CA and the diffusive base-aqueous proton encounter to form H^+B. In equation (8), $k_{dis(HB)}$ is the H^+B's acid dissociation rate constant and $k_{D(HB)}$ is the diffusion-limited rate constant of the back protonation of B to reform H^+B. R_i is the main protonation route for strong, i.e. readily dissociating, acids.

Generation of kinetic plots in Figure 3. We now ask – in connection with our experimental results for CA's protonation viability shown in Fig. 2 –which of CA's two protonation routes – direct R_d or indirect R_i – is more important. We also check the possibility of the base catalyzing the decomposition of CA before it is able to protonate the base, the R_{ic} route with the k_{ic} second order reaction rate constant [cf. equation (4)]. This is accomplished by numerically solving the following set of rate equations covering the CA-base kinetic scheme described above:

$$d[H_2CO_3]/dt = -k_{on}[H_2CO_3][B]+k_{off}[HCO_3^-][H^+B]+k_{D(BC)}[HCO_3^-][H^+]-k_{dis(CA)}[H_2CO_3]-k_{ic}[H_2CO_3][B]-k_{dc}[H_2CO_3]$$

$$d[HCO_3^-]/dt = k_{on}H_2CO_3][B]-k_{off}[HCO_3][H^+B]-k_{D(BC)}[HCO_3^-][H^+]+k_{dis(CA)}[H_2CO_3] \qquad (9)$$

$$d[H^+]/dt = -k_{D(HB)}[H^+][B]+k_{dis(HB)}[H^+B]-k_{D(BC)}[HCO_3^-][H^+]$$

$+k_{dis(CA)}[H_2CO_3]$

$d[B]/dt = -k_{on}H_2CO_3][B]+k_{dis(HB)}[H^+B]+k_{off}[HCO_3^-][H^+B]$
$-k_{D(HB)}[H^+][B]$

(We have neglected the reaction $CO_2 + OH^- \rightleftarrows HCO_3^-$ since the OH^- concentration will be negligible in the strongly acidic pH ~ 3.5 experimental solutions.)

For the various rate constants in this reaction listing, the diffusion-controlled rate constants $k_{D(B)}$, $k_{D(BC)}$, $k_{D(HB)}$ and the rate constants k_{off}, $k_{dis(CA)}$ and $k_{dis(HB)}$ for the direct route parameters and for the indirect route parameters are available (SI Appendix, Tables S1 and S2 respectively). The unimolecular rate constants' values for CA decomposition to H_2O and CO_2 are k_{dc} (20^oC) = 19.5 s^{-1} and $k_{dc}(5^oC)$ = 5.5 s^{-1}, determined independently by conventional one-stage stopped-flow experiments (SI Appendix, sec. S7).

The first conclusion is that, as noted above, the full numerical solutions of the kinetic scheme rate equation (9) set confirm the conclusions we previously reached for Fig. 2. The detailed mechanistic question requires a bit more analysis. The relatively long timescale of the Fig. 2 experiments cannot directly provide the reaction mechanisms for the too rapid protonation time dependence; nonetheless, our kinetic scheme provides such mechanistic information by comparing the scheme's predictions for the limiting protonated base concentration value reached in the experiments. The detailed kinetic protonation profile results for assorted mechanistic possibilities displayed in Fig. 3 for the 14NS base (and also for the HPTS base (SI Appendix, Fig. S3)) show by this comparison (cf. the red arrow in Fig. 3) that the direct protonation route R_d dominates the protonation reaction, and – more generally and importantly – that the base protonation by CA must be *fast* compared to the decomposition to H_2O and CO_2, equation (2) –which can be neglected – and further, that there is negligible base-induced decomposition via equation (4).

Figure 3 contains even further information concerning CA's protonation ability and mechanisms. We first note that the Fig. 2 experimental protonation yield (with respect to intact CA's initial concentration) approaches 100%; thus practically all of the CA acidic protons were transferred to the base, quantitatively protonating it. As mentioned above, the Fig. 3 calculations show that the direct protonation R_d route largely dominates over the indirect protonation route R_i (assuming R_d is diffusion-limited), consistent with the behavior of any Brønsted acid of CA strength protonating a strong base. This domination means that under Fig. 2's conditions, the intact CA-base encounter is much faster than the encounter between the base and those $(H^+)_{aq}$ protons generated by CA dissociation. It further means that CA's direct protonation of the base largely precedes its proton dissociation equation (3); thus, the important conclusion is that most protonation reactions in our experiments have occurred by intact CA.

Figure 3 displays other reaction possibilities. In the more significant one of these, we consider the potential "short circuiting "of R_d by the CA-B encounter route equation (3), where intact CA does not protonate the base, and the encounter instead results in CA decomposing to CO_2 and H_2O. Figure 3 indicates that this mechanism may only account for about 17% of the observed protonation yield. In view of this and the remaining Fig. 3 calculation results, as well as the discussion of the experimental Fig. 2, we can conclude that it is highly unlikely that CA appreciably decomposes as a result of encountering a base.

It is worth mentioning that our CA protonation rate constant observations are in complete harmony with our detailed ab initio CA protonation reaction mechanism, which predict ultrafast protonation rates of strong nitrogen bases without any base-induced CA decomposition (57, 58).

Specifically, Car-Parrinello molecular dynamics simulations in an aqueous environment demonstrated that CA's protonation of methylamine base CH_3NH_2 within a hydrogen (H)-bonded complex occurs extremely rapidly: the path for the practically barrierless PT from CA to methylamine within such a complex was fully mapped and the computed extremely short time scale (33−75 fs) protonation occurred without CA decomposition. The PT process is strongly downhill in free energy character ($\Delta pK_a \approx 7$), consistent with the current assessments of the pK_a values of 3.5 (42) and 10.6 for CA and protonated methylamine respectively (57,58). Further, in additional studies we have found similar PT reaction rates when CA and the base are bridged by a single H-bonded water molecule.

Relevance for human physiology and marine biology. The present experimental studies have substantial relevance for human physiology, and their consequences are clear. Our findings, supported by previous theoretical results, demonstrate that intact carbonic acid (CA) is an efficient protonation agent and unequivocally justify the inclusion of CA as a key factor in the physiological 'book-keeping' of available protons in the blood plasma acting as an essential (reversible) part of the bicarbonate/ CO_2 buffer. This inclusion of intact CA as an important physiological ingredient in the bicarbonate/CO_2 buffer addresses the important physiological problem described in the Introduction: it enables the significant bridging of the reactivity gap between the fast protonation rates needed to maintain many physiological processes and the insufficient supply of hydrated protons present at the normal physiological pH = 7.4.

Our results indicate that maintenance of the CA concentration within the normal physiological 2-3 μm range is sufficient for CA – either directly or non-directly (by H^+ generated by CA's dissociative PT to the water solvent) – to perform several key functions. CA will not only assist maintaining the physiological pH balance; it will also directly protonate practically any nearby physiological base (either neutral or negatively charged) which requires transient protonation in order to effect its biological activity. In this connection, Fig. 4 displays – using the model reaction scheme equations described in its caption – the non-enzymatic protonation of a histidine-like residue by either the steady-state concentration of $(H^+)_{aq}$ in physiological-like conditions or directly by intact CA. [Histidine residues serve as proton 'antennas' in biological environment collecting protons and then transferring them to a reaction center; cf His 64 in the carbonic anhydrase complex (59).] Although the actual protonation rates will be affected by the specific local conditions of the blood-plasma, there is a clear message of Fig. 4: that protonation by intact CA is much faster than protonation by $(H^+)_{aq}$ and, in consequence, that efficiently fast protonation reactions in biological environments are not necessarily enzymatic. This last conclusion does not follow for protonation solely by $(H^+)_{aq}$, which at its physiological steady-state concentration of $4x10^{-8}$ M will have typical protonation times in the ms range.

The situation is similar for marine biology. In the oceans, the pH is even lower than in the blood, only about 8.05 compared to 7.40, and the bicarbonate concentration is also substantial, about 2 mM. Consequently, the CA concentration is 2-3 times larger than $[H^+]_{aq}$ there and provides the stable pH conditions upon which most marine life's well-being depends (10-15). Comprehension of intact CA's chemistry will be necessary to assess the full impact on marine life of ocean acidification driven by atmospheric CO_2 concentration increase (12,13). Marine organisms with a calcium skeleton such as corals illustrate the issues here. Such skeletons structurally weaken when the oceans become more acidic (14,15). Taking CA into account will approximately double the ocean acidification effect of $(H^+)_{aq}$ alone (15). Such additional contributions of CA will undoubtedly increase the projected negative effect of ocean acidification on marine life.

Conclusions. The present work indicates that CA is an important factor in the body's ability to maintain the large fluxes of protons and high protonation rates which are absolutely vital to sustain metabolic life-supporting processes and rapid enzymatic reactions. In particular, our findings identify CA as a significant source of protons readily available for these tasks with high kinetic efficiency. The non-vanishing presence of this small, mobile (neutral) carboxylic acid, which is strong enough to rapidly protonate practically all protonatable basic groups in human blood which then continue to react in their acid form – should not be ignored or marginalized.

Our findings also unveil the outstanding advantage of Nature's choice of the CA buffer as its leading buffer: dynamically, CA is a much stronger acid than all the secondary buffers in the blood plasma. As such, CA acts as a fast-release proton storage with an overall bimolecular protonation rate of typical biological bases much larger than $(H^+)_{aq}$'s. CA has a further advantage: it would be able to directly protonate weak biological bases such as Histidine (pK_a (H^+B) = 6.0) that are slow to protonate by secondary mobile buffers constructed with acids much weaker than CA; examples include H_2PO_4 (pK_a = 6.8), peptides, small proteins with pK_as in the 6-9 pK_a range, and carboxylate side-groups with typical pK_a values of 4-6 such as in the important drug Ibuprofen. Such drug molecules may be transiently protonated by the stronger CA while diffusing in the blood plasma (60). Clearly, further investigations are needed to fully assess CA's physiological importance. It should be revealing to determine how CA reacts and protonates bio-relevant bases in environments other than pure water. We expect that in such environments – especially in aprotic polar ones such as pure DMSO – CA will become much more stable, with its lifetime increasing from the ms to the s range. In such environments CA's direct protonation efficiency should remain high. Our preliminary experiments indicate the validity of these expectations.

Methods

Stopped-flow UV–visible experiments were performed using BioLogic SFM-3000 stopped-flow spectrometer (Bio-Logic SA, Claix, France).

The stopped-flow, two-stage rapid mixing, experimental investigation (Fig. 5) was carried out as follows. In the apparatus' first mixing cell, CA was transiently generated by mixing HCl with sodium bicarbonate $NaHCO_3$. The solution in the mixing cell where CA was prepared was incubated and allowed to fully equilibrate in the mixing cell (1 ms mixing time) for at least 2 ms and up to 1 s before the intact CA was mixed with, and protonated the base in, the base solution in the second mixing cell. Longer incubation times resulted in CA appreciably decomposing to CO_2 and H_2O prior to reacting with the base: the longer the incubation time, the more the CA's initial concentration was reduced by its decomposition in the first mixing stage.

For these two-stage mixing experiments, the first mixing stage is described in the SI Appendix for the conventional one step mixing experiments, while the second stage involved mixing of CA and one of the two representative bases, the HPTS or 1N4S bases. The base's UV-VIS absorption served as its concentration indicator. When mixed with the base in the second mixing chamber, the base protonation reaction was completed practically instantaneously on the 1 ms mixing time-scale, and this protonation reaction is governed by the CA concentration at the time of mixing established by the incubation time in the first chamber where CA was generated.

Acknowledgment

This work has been supported by NIH Grant PO 1000125420 (JTH, EP).

References

1. Markert CL & Møller F (1959) Multiple forms of enzymes: Tissue, ontogenetic, and species specific patterns. *Proc Natl Acad Sci USA* 45(5):753-763.

2. Warshel A & Russell S (1986) Theoretical correlation of structure and energetics in the catalytic reaction of trypsin. *J Am Chem Soc* 108(21):6569-6579.
3. Adrogué HJ & Madias NE (2016) Assessing acid-base status: Physiologic versus physicochemical approach. *Am J Kidney Dis* 68(5):793-802.
4. Lee M, Bai C, Feliks M, Alhadeff R, & Warshel A (2018) On the control of the proton current in the voltage-gated proton channel HV1. *Proc Natl Acad Sci USA* 115(41):10321.
5. Junge W & McLaughlin S (1987) The role of fixed and mobile buffers in the kinetics of proton movement. *Biochim Biophys Acta, Bioenerg* 890:1.
6. Vaughan-Jones RD, Spitzer KW, & Swietach P (2006) Spatial aspects of intracellular pH regulation in heart muscle. *Prog Biophys Mol Biol* 90:207.
7. Schmidt RF & Thews G eds (1980) *Human physiology* (Springer-Verlag, Berlin).
8. Waugh A & Grant A (2007) *Anatomy and physiology in health and illness* (Churchill Livingstone Elsevier) Tenth Ed p 22.
9. Geers C & Gros G (2000) Carbon dioxide transport and carbonic anhydrase in blood and muscle. *Physiol Rev* 80:681.
10. Millero FJ (2007) The marine inorganic carbon cycle. *Chem Rev* 107:308.
11. Fietzke J, *et al.* (2015) Century-scale trends and seasonality in pH and temperature for shallow zones of the bering sea. *Proc Natl Acad Sci USA* 112(10):2960-2965.
12. Maher K & Chamberlain CP (2014) Hydrologic regulation of chemical weathering and the geologic carbon cycle. *Science* 343:1502-1504.
13. Hansen J & Sato M (2004) Greenhouse gas growth rates. *Proc Natl Acad Sci USA* 101 (46):16109-16114.
14. Tresguerres M & Hamilton TJ (2017) Acid-base physiology, neurobiology and behaviour in relation to CO_2 induced ocean acidification *J Exp Biol* 220:2136-2148.
15. Mollica NR, *et al.* (2018) Ocean acidification affects coral growth by reducing skeletal density. *Proc Natl Acad Sci USA* 115(8):1754-1759.
16. Scanlon VC & Sanders T (2003) *Essentials of anatomy and physiology*. (F.A. Davis Company) 7th Ed.
17. Thibodeau GA & Patton KT (2003) *Anatomy and physiology*. (St Louis, Mosby) 17th Ed.
18. Silverman DN & McKenna R (2007) Solvent-mediated proton transfer in catalysis by carbonic anhydrase. *Acc Chem Res* 40(8):669-675.
19. Supuran Claudiu T (2016) Structure and function of carbonic anhydrases. *Biochem J* 473(14):2023.
20. Dash RK & Bassingthwaighte JB (2006) Simultaneous blood-tissue exchange of oxygen, carbon dioxide, bicarbonate, and hydrogen ion. *Ann Biomed Eng* 34(7):1129-1148.
21. Mangan NM, Flamholz A, Hood RD, Milo R, & Savage DF (2016) pH determines the energetic efficiency of the cyanobacterial CO_2 concentrating mechanism. *Proc Natl Acad Sci USA* 113(36):E5354-E5362.
22. Wagner JP, *et al.* (2016) Tunnelling in carbonic acid. *Chem Commun* 52(50):7858-7861.
23. Mills GA & Urey HC (1940) The kinetics of isotopic exchange between carbon dioxide, bicarbonate ion, carbonate ion and water. *J Am Chem Soc* 62:1019-1026.
24. Roughton FJW (1941) The kinetics and rapid thermochemistry of carbonic acid. *J Am Chem Soc* 63:2930-2934.
25. Ho C & Sturtevant JM (1963) Kinetics of hydration of carbon dioxide at 25 degrees. *J Biol Chem* 238(10):3499-3501.

26. Gibbons BH & Edsall. JT (1963) Rate of hydration of carbon dioxide and dehydration of carbonic acid at 25 degrees. *J Biol Chem* 238:3502-3507.
27. Soli AL & Byrne RH (2002) CO_2 system hydration and dehydration kinetics and the equilibrium CO_2/ H_2CO_3 ratio in aqueous nacl solution. *Mar Chem* 78:65- 73.
28. Wang X, Conway W, Burns R, McCann N, & Maeder M (2010) Comprehensive study of the hydration and dehydration reactions of carbon dioxide in aqueous solution. *J Phys Chem A* 114:1734-1740.
29. Nguyen MT, Raspoet G, Vanquickenborne LG, & Van Duijnen PT (1997) How many water molecules are actively involved in the neutral hydration of carbon dioxide? *J Phys Chem A* 101(40):7379-7388.
30. Loerting T, *et al.* (2000) On the surprising kinetic stability of carbonic acid (H_2CO_3). *Angew Chem, Int Ed Engl [Angew Chem]* 39 [112](5):891-894 [918-922].
31. Tautermann CS, *et al.* (2002) Towards the experimental decomposition rate of carbonic acid (H_2CO_3) in aqueous solution. *Chem Eur J* 8(1):66-73.
32. Lewis M & Glaser R (2003) Synergism of catalysis and reaction center rehybridization. A novel mode of catalysis in the hydrolysis of carbon dioxide. *J Phys Chem A* 107:6814.
33. Kumar PP, Kalinichev AG, & Kirkpatrick RJ (2007) Dissociation of carbonic acid: Gas phase energetics and mechanism from ab initio metadynamics simulations. *J Chem Phys* 126(20):204315.
34. Nguyen MT, *et al.* (2008) Mechanism of the hydration of carbon dioxide: Direct participation of H_2O versus microsolvation. *J Phys Chem A* 112(41):10386-10398.
35. Marx D (2006) Proton transfer 200 years after von Grotthuss: Insights from ab initio simulations. *Chemphyschem* 7(9):1848-1870.
36. Weller A (1961) Fast reactions of excited molecules *Progr React Kinet* 1:187-214.
37. Eigen M (1964) Proton transfer, acid-base catalysis, and enzymatic hydrolysis. Part i: Elementary processes. *Angew Chem, Int Ed Engl* 3:1.
38. Eigen M, Kruse W, Maass G, & DeMaeyer L (1964) Rate constants of protolytic reactions in aqueous solution. *Prog React Kinet* 2:285.
39. Eigen M & Hammes GG (1963) Elementary steps in enzyme reactions (as studied by relaxation spectrometry). in *Advances in Enzymology and Related Areas of Molecular Biology*, ed Nord FF (John Wiley & Sons, Inc.), pp 1-38.
40. Brønsted JN (1923) Some observations about the concept of acids and bases. *Recueil des Travaux Chimiques des Pays-Bas* 42 (8):718–728.
41. Adamczyk K, Premont-Schwarz M, Pines D, Pines E, & Nibbering E (2009) Real-time observation of carbonic acid formation in aqueous solution. *Science* 326(5960):1690-1694.
42. Pines D, *et al.* (2016) How Strong is Carbonic Acid? *J Phys Chem B* 120:2440−2451.
43. Atkins P & de Paula J (2010) *Physical chemistry* (Oxford University, Oxford) Ninth Ed.
44. Kim MHK, C. S.; Lee, H. W.; Kim, K. (1996) Temperature dependence of dissociation constants for formic acid and 2,6-dinitrophenol in aqueous solutions up to 175 [degree]c. *J Chem Soc, Faraday Trans* 92(24):4951-4956.
45. Harned HS & Ehlers RW (1933) The dissociation constant of acetic acid from 0 to 60" centigrade. *J Am Chem Soc* (55):652-655.
46. Harned HS & Embree ND (1934) The temperature variation of ionization constants in aqueous solutions. *J Am Chem Soc* 56:1042.
47. Harned HS & Owen BB (1958) *The physical chemistry of electrolyte solutions* (Reinhold, New York) 3rd Ed.

48. Wissbrun KF, French DM, & Patterson A (1954) The true ionization constant of carbonic acid in aqueous solution from 5 to 45. *J Phys Chem* 58:693-695.
49. Tanaka M, Nomura H, & Kawaizumi F (1992) A simple method for evaluation of enthalpy of proton dissociation in water. *Bull Chem Soc Jpn* 65:410-414.
50. Pines E, Manes BZ, Lang MJ, & Fleming GR (1997) Direct measurement of intrinsic proton transfer rates in diffusion-controlled reactions. *Chem Phys Lett* 281(4-6):413-420.
51. Mohammed OF, Pines D, Pines E, & Nibbering ETJ (2007) Aqueous bimolecular proton transfer in acid-base neutralization. *Chem Phys 341*:240-257.
52. Kiefer PM & Hynes JT (2002) Nonlinear free energy relations for adiabatic proton transfer reactions in a polar environment. I. Fixed proton donor-acceptor distance. *J Phys Chem A* 106:1834.
53. Kiefer PM & Hynes JT (2002) Nonlinear free energy relations for adiabatic proton transfer reactions in a polar environment. II. Inclusion of the hydrogen bond vibration. *J Phys Chem A* 106:1850.
54. Pines E (2003) Uv-visible spectra and photoacidity of phenols, naphthols and pyrenols. *Chemistry of phenols* ed Rappoport Z (Wiley, New York), pp 491-529
55. Premont-Schwarz M, Barak T, Pines D, Nibbering ETJ, & Pines E (2013) Ultrafast excited-state proton-transfer reaction of 1-naphthol-3,6-disulfonate and several 5-substituted 1-naphthol derivatives. *J Phys Chem B* 117(16):4594-4603.
56. Lehninger AL (1976) *Biochemistry* (Worth Publishers, Inc., New York, NY).
57. Daschakraborty S, *et al.* (2016) Reaction mechanism for direct proton transfer from carbonic acid to a strong base in aqueous solution I: Acid and base coordinate and charge dynamics. *J Phys Chem B* 120(9):2271-2280.
58. Daschakraborty S, *et al.* (2016) Direct proton transfer from carbonic acid to a strong base in aqueous solution II: Solvent role in reaction path. *J Phys Chem B* 120(9): 2281–2290.
59. Fisher SZ, *et al.* (2007) Speeding up proton transfer in a fast enzyme: Kinetic and crystallographic studies on the effect of hydrophobic amino acid substitutions in the active site of human carbonic anhydrase II. *Biochemistry* 46(12):3803-3813.
60. Herzfeldt CD & Kümmel R (1983) Dissociation constants, solubilities and dissolution rates of some selected nonsteroidal antiinflammatories. *Drug Dev Ind Pharm* 9(5):767-793.

Figure Captions

Fig.1. Temperature dependence of the pK_a of CA. CA's pK_a was measured in the 5-37^oC range using a one-stage stopped-flow arrangement (27) (SI Appendix, Fig. S4) with CA generated within about 1 ms by mixing equal amounts of sodium bicarbonate $NaHCO_3$ and hydrochloric acid HCl. The solution's pH was determined by the absorption change of 2,4-dinitrophenol (DNP) (pK_a = 4.07 ± 0.02 at 20^oC), with its value's T-dependence accurately known (44). Points are the averaged pK_a values of at least 5 independent experiments; the solid line is the fit to equation (6). pK_a values were found (SI Appendix, equation S7.1) and then extrapolated to I=0. Error bars directly determined from the experimental result's total spread are ± 0.02 pK_a units.

Fig. 2. Fraction of protonated base (anions of HPTS and 1NS4) versus incubation time τ_{inc}. Time dependence of the experimentally observed fractions (points) of the anionic bases HPTS and 1NS4 protonated by CA vs the incubation time τ_{inc}, the time elapsed from the moment CA was

generated by HCl-bicarbonate reaction until it is mixed (duration τ_{mix} until the solution is homogeneous) with the base solution (see Methods for experimental setup description). During incubation, the CA concentration decreases continuously with a temperature-dependent exponential lifetime τ_{dc} (solid and dashed lines) due to its spontaneous decomposition via equation (2). τ_{dc} is independently determined to be on the tens of ms timescale by standard stopped flow experiments (SI Appendix, Fig. S4) (27, 28). The protonated base fraction decreases with increased τ_{inc} because of CA's spontaneous decomposition. Protonation is evidently spontaneous and much faster than τ_{mix} and τ_{dc} timescales (see text).

Fig. 3. Calculated kinetic profiles of the rise of the absorption of protonated 1N4S base via the numerical solution of equations (9). The simulated kinetic profiles are compared with the experimental absorption signal of 3.7 mM 1N4S after mixing with 1:1 3.5 mM buffer solution of CA/HCO^-_3. Red arrow: the stopped flow experiment's observed protonated base concentration after mixing with CA. The arrow also marks the predicted protonated base's concentration assuming full quantitative protonation by CA. Solid line: Both R_d [equation (1] and R_i routes [equation (8)] of the base protonation are active. Dotted line: Protonation by $(H^+)_{aq}$ without participation of any CA protonation reactions. The indirect protonation via $(H^+)_{aq}$ is treated as diffusion-limited (SI Appendix, sec.S4). Dashed line: assuming that CA indirectly, but not directly, protonates the base *and* decomposes upon encountering a base molecule according to equation (4). Dot-dot-dash line: assuming only the indirect protonation route R_i. Short-Dash line: solution assuming only the direct protonation route R_d; this is almost *indistinguishable* from the Solid line where both CA's direct and indirect protonation routes R_d and R_i are active. Similar analysis and conclusions apply for the HPTS base (SI Appendix, sec. S3).

Fig. 4. Transient protonation profiles of ahistidine-like base (59) B ($pK_a(H^+B) = 6.0$) in the presence of the CA/bicarbonate buffer. The two protonation reaction profiles are for the direct protonation reaction R_d by CA, $H_2CO_3 + B \rightarrow HCO_3^- + H^+B$ and for protonation by the equilibrium $(H^+)_{aq}$ protons, $(H^+)_{aq} + B \rightarrow H^+B$, assuming unidirectional protonation (since on the low- μs time-scale the opposite reactions are not significant). Calculated using $k_{D(B)} = 3x\ 10^9\ M^{-1}s^{-1}$ and $k_{D(HB)} = 1.5 \times 10^{10}\ M^{-1}s^{-1}$, for the physiological-like conditions pH = 7.4, $[HCO_3^-] = 25mM$, $[H_2CO_3] = 2.6\mu M$ and [B] = 10 nM. Profiles are displayed only up to the time that the protonated base reaches its steady-state concentration at the physiological pH =7.4. The initial direct protonation rate by the CA buffer is about 12 times larger than the initial protonation rate by $(H^+)_{aq.}$

Fig. 5. The two-stage stopped-flow setup used for the determination of CA's ability to protonate bases as shown in Fig. 2. In the first cell (top left), CA was generated by rapid acidification by HCl of bicarbonate anion HCO_3^-, resulting in a buffered solution with known pH. Following a variable incubation (delay) time during which there is a partial loss of CA due to spontaneous decomposition equation (1), the resulting CA solution was mixed in the second mixing cell (right) with the base solution, allowing protonation of the base by CA. Temperature was controlled to within $\pm\ 0.1^0$ C by a variable-temperature water circulator. The concentration of the protonated base was measured by absorption spectroscopy.

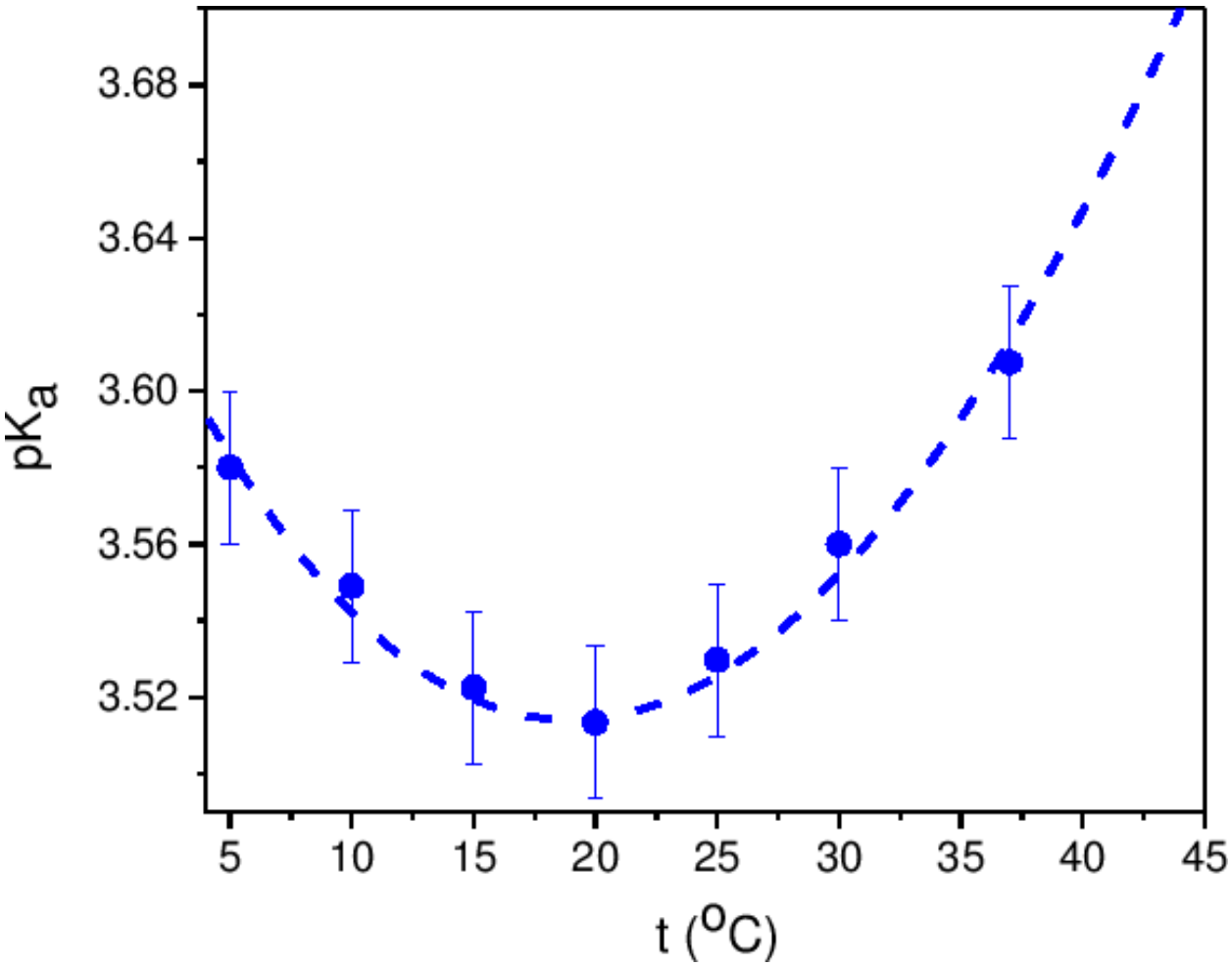
3.68
3.64
3.60
3.56
3.52
pKa
5
10
15
20
25
30
35
40
45
t (°C)

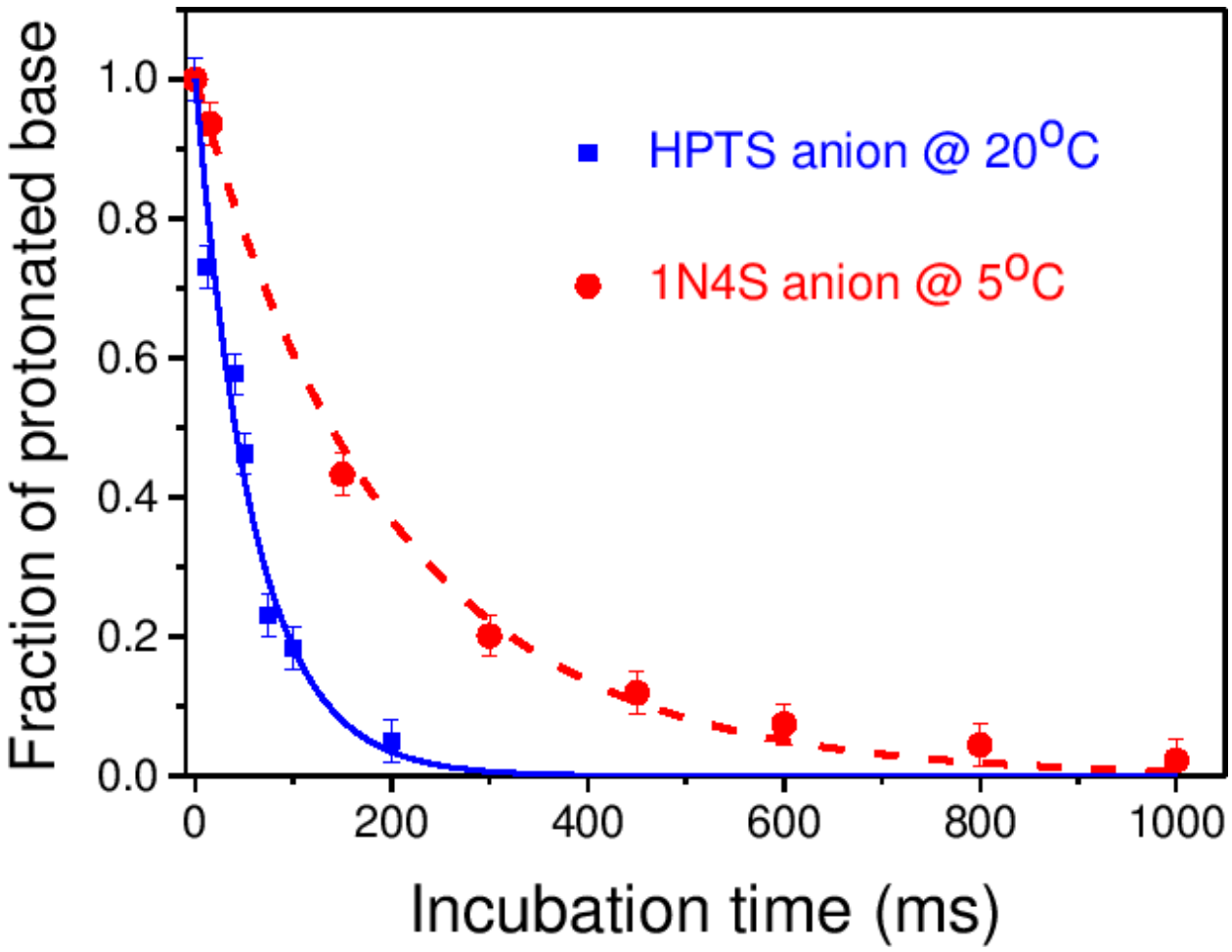
Fraction of protonated base
1.0
0.8
0.6
0.4
0.2
0.0
0
200
400
600
800
1000
Incubation time (ms)
HPTS anion @ 20°C
1N4S anion @ 5°C

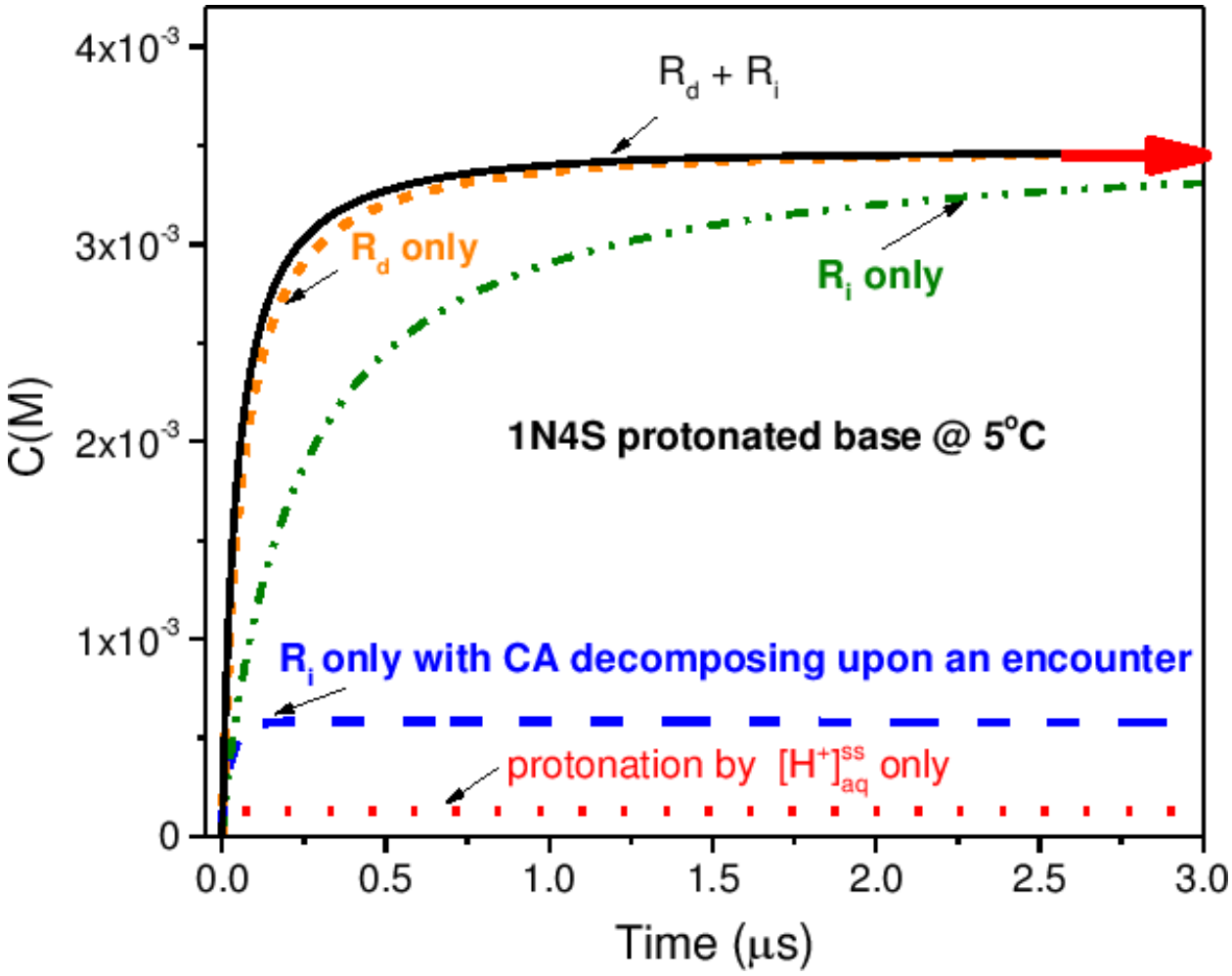
4x10-3
3x10-3
2x10-3
1x10-3
0
C(M)
0.0
0.5
1.0
1.5
2.0
2.5
3.0
Time (μs)
Rd + Ri
Rd only
Ri only
1N4S protonated base @ 5°C
Ri only with CA decomposing upon an encounter
protonation by [H+]ssaq only

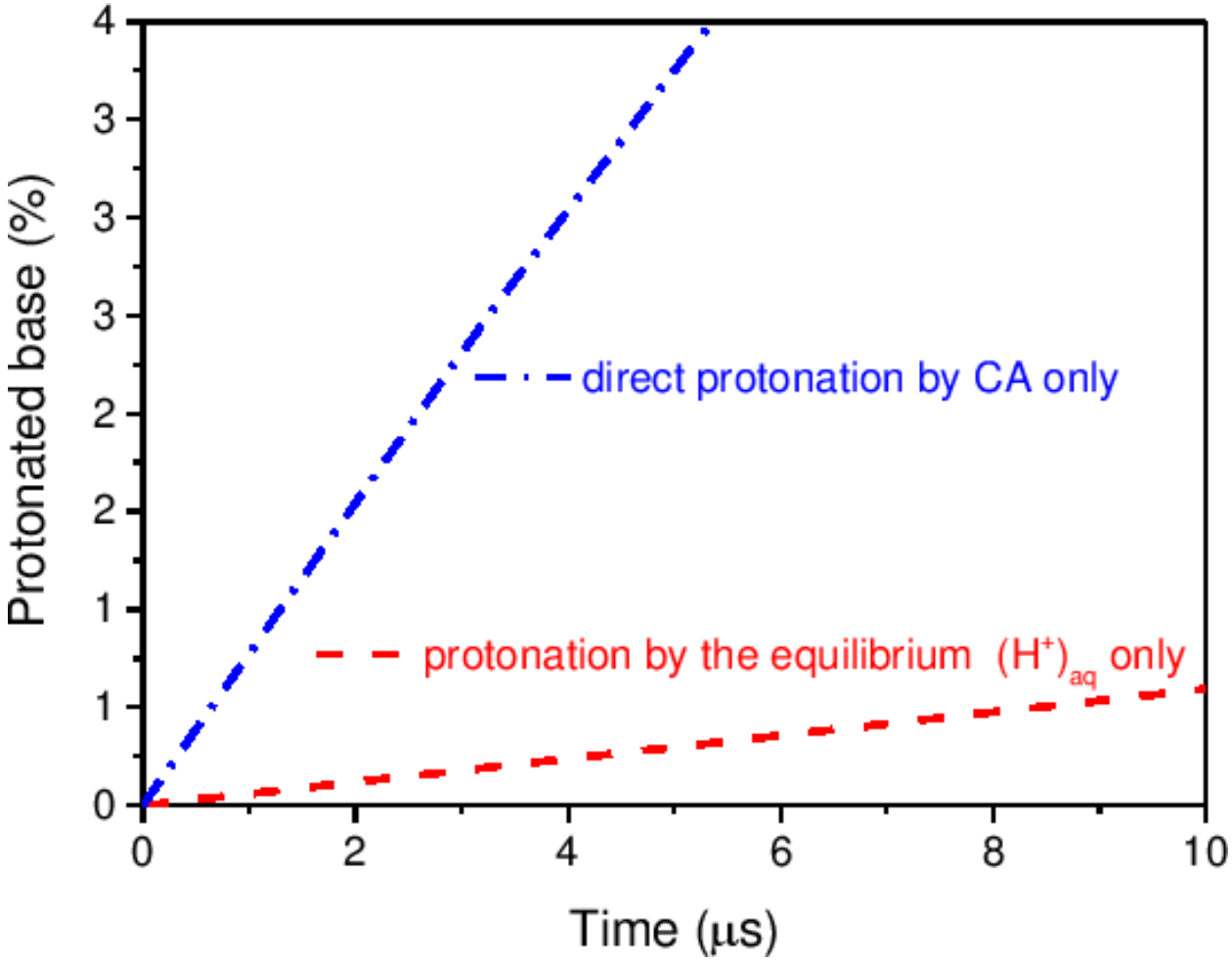
Protonated base (%)
Time (μs)
direct protonation by CA only
protonation by the equilibrium $(H^+)_{aq}$ only
0
1
1
2
2
3
3
4
0
2
4
6
8
10

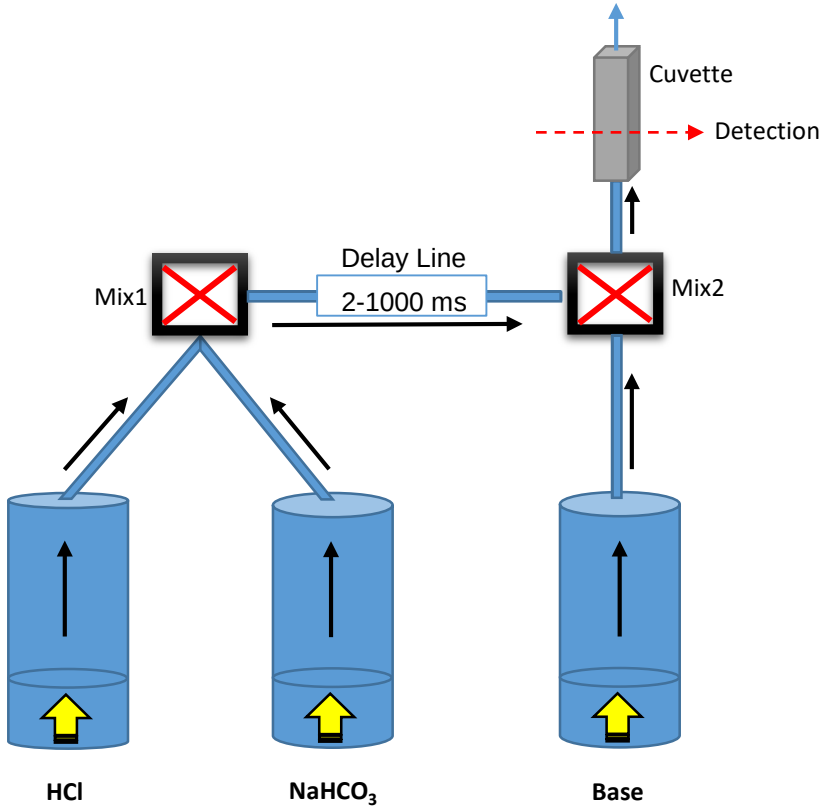
Cuvette
Detection
Delay Line
2-1000 ms
Mix1
Mix2
HCl
NaHCO3
Base

PNAS
www.pnas.org

Supplementary Information for

Carbonic Acid: A viable protonating agent for biological bases

Daniel Aminov[a], Dina Pines[a], Philip M. Kiefer[b], Snehasis Daschakraborty[b], James T. Hynes[b,c], and Ehud Pines[a]

Ehud Pines
Email: epines@bgu.ac.il

This PDF file includes:

Supplementary text
Figs. S1 to S4
Tables S1 to S2
References for SI reference citations

Introductory Remarks. As explained in the main text section "***Testing the kinetic viability of CA as a protonating agent***", the kinetics of potential base protonation routes for Carbonic Acid (CA) ─ while obviously an essential aspect of the assessment of CA's practical functioning as an acid ─ are not known, mainly because of CA's thermodynamic instability [see e.g. main text equation (2)]. In this SI, we give ─ by an analysis of CA's base protonation reactions ─ more detail on the description of these protonation routes, including the determination/estimation of the various constants necessary for their evaluation.

After this is done, we then need to connect these protonation routes to the experimental results in main text Fig. 2. However, this connection is not straightforward, because the slow time scale of the key base protonation stopped-flow experiment in main text Fig. 2 unfortunately does not permit the experimental following in real time of the protonation kinetics. Nonetheless, we can connect the experimental results to the protonation reactions' kinetics in a different fashion, as was done in main text Fig. 3. In particular, this connection requires the incorporation of the protonation schemes into a detailed kinetic scheme ─ also including CA's acid dissociation and decomposition reactions, main text equations (2-4) ─ in order to correctly predict the experimental long time protonated base yield available from the experimental Fig. 2 results.

The outline of this SI is then as follows. Some general aspects of the two protonation mechanisms themselves are discussed in Sec. S1. Next, the protonation reaction rate equations that we will use in our analysis of the experimental Fig. 2 of the text are justified in Sec. S2 [equations (S2.3) and (S2.5)]. The following Sections S3 and S4 then deal with the analysis of these equations for the direct and indirect protonation mechanisms respectively, as well as the determination of the reaction parameters needed for the experimental results' analysis. Section S5 deals with an additional decomposition route for CA included in the scheme. Section S6 provides a detailed discussion of the results of the detailed kinetic scheme of coupled reactions [equation (9)]employed to generate model predictions for text Figs. 2-4, as well as for Fig. S3, which is the HPTS (8-hydroxy-1,3,6-trisulfonate) analogue of the text Fig. 3 for the base IN4S (1-naphthol-4-sulfonate); comments on the dominance of the direct protonation route are also offered here. Finally, the stopped flow set-up and experimental procedures are described in Sec. S7.

In closing these introductory remarks, we note that the combination of the SI's entire discussion of CA's reactions, i.e. its protonation mechanisms and other reactions including decomposition, and the description of the associated full kinetic analysis necessary for the interpretation of the experimental text Fig. 2 (as well as the related text Figs. 3 and 4) is rather long and detailed, requiring Secs. S1-S6. It is thus useful to succinctly anticipate several of its major conclusions here. First, the base-induced decomposition route text equation (4) for CA is unimportant and can be ignored, as is the decomposition text equation (2), a conclusion crucial for the viability of CA as a protonating agent. Second, in timescale and mechanism, CA should be able to protonate biologically relevant bases with an efficiency similar to that of regular carboxylic acids of a comparable pK_a (among which is the biologically important lactic acid (5)). This should make CA an important protonation agent in the blood plasma, either by direct proton transfer to a nearby base or indirectly via its acid dissociation reaction generating $(H^+)_{aq}$ which will then protonate a nearby base (see further discussion in S1 below).

S1. CA Protonation Routes Overview. We examine two main limiting protonation routes of CA, typical for general acid-base reactions ─ whose forms equations (1) and (8) of the main text were discussed and modelled by Weller and Eigen (6-9). (We generally refer to this kinetic model as the EW model, of which there are several variants see e.g. Refs (6-9)).

The *direct* protonation route R_d is suitable for describing the acid-base reactivity of acids which encounter and protonate a base B without prior appreciable proton-dissociation, i.e. transfer of their proton to a solvent water molecule. The *indirect* protonation route R_i is suitable for

describing strong acids which protonate a base B through protons $(H^+)_{aq}$ that have already transferred by the acid to the water solvent, i.e. the case when ─ instead of the acid ─ it is a protonated water solvate moiety that protonates B. In the above, we are considering that the base is either charged or with no charge, and. Here and below, we denote the base simply as 'B' without indication if it is charged or neutral.

The above two routes will be our primary focus, but for completeness we also need to include a possible third reaction route R_{ic} for CA which provides a CA loss route in addition to text equation (2). In this R_{ic} route, given by text equation (4), CA decomposes ─ before any acid PT to the base ─ as a result of encountering the base: upon encountering CA, the base catalyzes the intact acid's bimolecular decomposition to form the unreactive products CO_2 and H_2O. If the rate of this base-catalyzed CA decomposition were diffusion (encounter)-limited, R_{ic} would result in CA disappearing from the solution much faster than solely by the first-order decomposition equation (2). This would result in diminishing CA's ability to directly protonate bases, effectively reducing CA's function in physiological environments to only a proton storage, releasing H^+ to water in order to maintain the proper physiological balance of $(H^+)_{aq}$.

S2. Eigen-Weller (EW) Reaction Model. We now employ the EW model (6-9) for the analysis of the protonation reaction routes R_d and R_i, equations (7) and (8) of the main text. Our discussion is geared to be relevant for our stopped-flow experiment, in particular, the case when an acid is introduced very rapidly into a homogeneous solution of the base. It may be viewed as a generalization of the EW model: the intact acid remains undissociated (typical of weak acids) until encountering the base by bulk diffusion, or the intact acid first dissociates to form the solvated proton $(H^+)_{aq}$ (typical of strong acids) which subsequently encounters the base via bulk.(6 - 8) One may view this situation as a competition between two parallel reactions of CA. The first is a unimolecular proton dissociation reaction of CA to the solvent and the second one a bimolecular proton transfer reaction between CA and a base molecule. The unimolecular reaction essentially progresses with a fixed timescale depending only on the environment; in contrast, the timescale of the bimolecular reaction will also depend on both the basicity and concentration of the base.

The direct route R_d will require by far the most extensive description, since we need to justify the simplified main text equation (7). To this end, we need to consider not simply CA's rate constant k_p for the unimolecular (contact) protonation $[B\cdots H_2CO_3]_a \xrightarrow{k_p} HCO_3^- + H^+B$, but instead CA's *overall* bimolecular protonation rate constant, which we label k_{on}. To obtain k_{on}, we employ the EW bimolecular two-stage reaction model involving three states: reactants, products, and intermediate reaction complexes. This description considers both the diffusion and the activation stages of a general bimolecular reaction in solution (6-9). The activation stage is further subdivided into several activation stages to preserve reversibility by introducing the back PT reaction within the reaction complex, with the first order rate constant k_{-p}: $HCO_3^- + H^+B \xrightarrow{k_{-p}} [B\cdots H_2CO_3]_a$.

With the above considerations, the EW reaction model for the direct PT reaction route R_d for CA is given by

$$H_2CO_3 + B \underset{k_S}{\overset{k_{D(B)}}{\rightleftharpoons}} [B\cdots H_2CO_3]_a \underset{k_{-p}}{\overset{k_p}{\rightleftharpoons}} [H^+B\cdots HCO^-_3]_a \underset{k'_D}{\overset{k'_S}{\rightleftharpoons}} HCO_3^- + H^+B \qquad \text{(S2.1)}$$

which is a more general form of equation (7). Here $k_{D(B)}$ and k'_D are the diffusion-limited rate constants for the reactants and products, while k_S and k'_S are the diffusion-limited rate constant for separating the reactants and products from contact-to bulk-separations (6-9). We can now justify text equation (7), since the reaction equation (S2.1) reduces to text reaction (7) for strong

proton-accepting bases having pK_a (HB) ≥ 6, a range typical of many physiologically important bases. In particular, for such strong base protonation reactions, k_p is very large and k_{-p} is very small, so that the contact proton transfer reaction from CA to the base may be treated as unidirectional, i.e. as text equation (7), repeated here for convenience:

$$H_2CO_3 + B \underset{k_S}{\overset{k_{D(B)}}{\rightleftharpoons}} [B \cdots H_2CO_3]_a \xrightarrow{k_p} H^+B + HCO_3^- \qquad \text{(S2.2)}$$

To summarize then, with this scheme, equation (S2.1) has been replaced by text equation (7) which is just equation (S2.2). Finally then, within the EW model, the overall two stage acid-base (forward) reaction for the direct route R_d, which we will use for our analysis of the forward reaction, is

$$H_2CO_3 + B \xrightarrow{k_{on}} H^+B + HCO_3^- \qquad \text{(S2.3)}$$

with rate constant k_{on}

$$k_{on} = k_{D(B)}k_p/(k_S + k_p) \qquad \text{(S2.4)}$$

which together are just the apparent steady-state results for the forward direction protonation reaction (S2.2). We recall the meaning of the various rate constants here: $k_{D(B)}$ is the diffusion-limited (bimolecular) CA-B encounter rate constant for a CA-B encounter, k_p is the unimolecular on-contact reaction rate constant for PT from CA to a base resulting from this encounter, and k_S is the separation constant. (An inclusion of a reverse reaction in addition to equation (S2.3) will be discussed in Sec. S3.)

The indirect protonation route reaction model equation (8), repeated here, is a combination of two one-stage acid dissociation reactions which are coupled by production and consumption of $(H^+)_{aq}$ in the H_2O solvent:

$$H_2CO_3 + B \underset{k_{D(BC)}}{\overset{k_{dis(CA)}}{\rightleftharpoons}} (H^+)_{aq} + HCO_3^- + B \underset{k_{dis(HB)}}{\overset{k_{D(HB)}}{\rightleftharpoons}} HCO_3^- + H^+B \qquad \text{(S2.5)}$$

In equation S2.5 the contact complexes, between H^+ and HCO_3^- ($[HCO_3^- \cdots H^+]_{aq}$, product side) and between H^+ and B ($[B \cdots H^+]_{aq}$, reactant side) are omitted. This is justified by the features that both protonation reactions involve protonation by $(H^+)_{aq}$ and as such are diffusion-limited with the complexes' and $[HCO_3^- \cdots H^+]_{aq}$ protonation reactions being much faster than the overall diffusion-controlled reactions.

S3. Direct Protonation Route R_d Analysis. We now consider the details of the rate constant equation (S2. 4) for the direct forward protonation reaction equation (S2.3). When CA protonates moderately strong and strong biological bases ($pK_{BH} > 6$, in which B now labels the biological base), k_p is very large compared to k_S, and the rate-determining step for the forward ('on') PT reaction from CA to the base is set by the bimolecular diffusive rate of encounter between these two reactants. In this limit, $k_S + k_p = k_p$ and the overall 'on' (irreversible) PT rate constant equation (S2.3) reduces to k_D, the diffusion-limited reaction rate constant,

$$k_{on} = k_D = 4\pi D_{AB} N' a \qquad \text{(S3.1)}$$

Here D_{AB} is the relative diffusion coefficient of the acid-base pair partners in cm^2/s^{-1} units, N' is $N_A/1000$ where N_A is Avogadro number and *a* is the contact radius, which for ordinary PT reactions is almost a constant $a = 5.5\pm1 \times 10^{-8}$ cm (6-9).

We can also determine if the important conclusion that the overall PT rate of the CA-biological base reaction is diffusion-limited (as we have just argued) by using equation (S3.1) and the Kiefer-Hynes perspective for the k_p - PT reaction free energy change relation (see Fig. S1), in which the reaction activation free energy $\Delta G_{rxn}^{\#}$ is calculated via a second-order expansion around the thermoneutral reaction free energy $\Delta G_{rxn}^{o} = 0$ (10-13). This correlation uses a reaction parameter, k_p (activationless) = $10^{12}s^{-1}$, a value known to well correlate the PT reaction rate of ultrafast acid-base reactions in aqueous solutions: in particular, this reaction rate pre-factor successfully correlates solvent-mediated contact PT rate constants for ordinary carboxylic acids and aromatic alcohols with their respective pK_as (14-17).

Turning to the prediction for CA and the biological bases, we first observe that the on-contact rate constant k_p of PT by CA in Fig. S1 depends upon the reaction free energy ΔG_{rxn}; it is very large – $k_p > 10^{11}s^{-1}$ – for protonating all sufficiently strong bases, i.e. those having a $pK_a > 6$. In bimolecular reactions such a large value for the contact reaction rate indicates that the overall reaction is in fact diffusion-limited. This important conclusion applied to our employed bases 1N4S and HPTS, where according to Fig. S1 the calculated k_p are $3x10^{11}s^{-1}$ and $4x10^{11}s^{-1}$ for 1N4S and HPTS respectively, values about 2 orders of magnitude larger than the diffusion-limited rate constant k_s for separating the reactant from contact- up to bulk-separations (6-9).

In summary, the overall PT reactions for the direct route R_d are diffusion-limited. Indeed, such very large k_p values for even mildly strong bases makes the overall bimolecular protonation by CA of most physiological bases diffusion-limited (6-9).

Our discussion above has focused exclusively on the forward direction of the base protonation by CA. In our numerical analysis of the protonation route R_d (leading to text Fig. 3), we generalize the description by complementing the forward equation (S2.3) by including the reverse direction as well: we adopt the general, reversible two-stage EW model (6-9) for the direct protonation route R_d for CA reaction (S2.1) by an effectively one stage (reversible) acid-base reaction text equation (1), repeated here

$$H_2CO_3 + B \underset{k_{off}}{\overset{k_{on}}{\rightleftharpoons}} HCO_3^- + H^+B \qquad \text{(S3.2)}$$

The rate constants here, k_{on} equation (S3.1) and k_{off}, cannot both have purely diffusion-limited values because k_p and k_{-p} in reaction (S2.1) cannot both be very large for the same acid-base pair. Thus, the *off* reaction must be activation-limited and its rate constant value will depend on its specific activation free energy**.**

We first consider the numerical evaluation of $k_{on} = k_{D(B)}$ via equation (S3.1). The reaction radius *a* is taken as 6 Å and D_{AB}, the acid-base reactive pair partners' relative diffusion coefficient is taken as $D_{AB} = D(H_2CO_3) + D(B)$ (Table S1). As for k_{off}'s numerical value, we exploit the fact that the equation (S3.2) reaction equilibrium constant (6-9) $K_{eq} = k_{on}/k_{off,}$ can be related to the ratio of the two acid dissociation equilibrium constants $K_a(CA)/ K_a(H^+B)$, so that we can write

$$k_{off} = k_{D(B)}/10^{\,pKa\,(HB)-\,pKa\,(CA)} \qquad \text{(S3.3)}$$

with the pK_a difference term providing the activation free energy contribution. k_{off} can thus be evaluated from the numerical values of k_{on} and the K_a's – of CA and of the base B's conjugate acid – for those acids' proton dissociation to water reactions (14-17). The resulting rate constants for the direct route equation (S3.2) are provided in Table S1.

In closing this sub section, we give several further supports for our key conclusion that k_{on} in equation (S3.2) must have its diffusion-controlled value for our direct route CA protonation reactions. Our first support exploits results from the protonation reaction of bicarbonate, the reverse, backward reaction in equation (S3.2). When this reaction is carried out in the case that BH^+ is much stronger acid than CA ($pK_{BH} < 1$), k_{off} is expected to be diffusion-limited while k_{on} is expected to be activation-controlled and hence to be much smaller than its diffusion-limited value. This was indeed found for the protonation of HCO_3^- by strong acids having a pK_a of about 0. (16, 17). In these excited-state PT reactions – for which PT to the bicarbonate base was strongly downhill in free energy, k_{off} in |equation (S3.2) was well-approximated by the theoretical k_D value using equation (S3.1), while k_{on} was much smaller than its diffusion-limited value and activation limited (i.e., the same logic as applied to our case, where the situation for forward and reverse directions is reversed).

Next, our numerical Car-Parinnello simulations for the reaction between CA and the strong methylamine base provide the second support (20, 21). These resulted in the intrinsic (i.e. contact, not solvent mediated) PT rate constant result $k_p > 10^{13}\ s^{-1}$ within the H-bonding complex between CA and the base (20, 21); this means that $k_{on} = k_D$ for strongly down-hill PT from CA, just as we have argued.

Finally, in a reaction series of PT from acetic acid to several nitrogen bases, Eigen et al. (7-9) demonstrated that acetic acid's PT approached the diffusion-controlled limit when the pK_a difference between acetic acid and the nitrogen base's conjugate acid was about 3.5 pK_a units; this difference is similar or smaller than the pK_a difference for the CA reactions analyzed in Fig. 3 in the main text, so that our conclusion is again supported.

S4. Indirect Protonation Route R_i. In the indirect route R_i for protonation by CA (equation (S2.5)), our discussion can be considerably more brief, because the base's protonation occurs only by $(H^+)_{aq}$. Here CA first proton-dissociates in the water solvent, likely first forming $(H_3^+O)_{aq}$ or $(H_5^+O_2)_{aq}$, and acting like a proton capacitor which steadily releases protons into the solution. These released protons then protonate the base, i.e. equation (S2.5).

The assorted rate constants appearing in equation (S2.5) were evaluated as follows. We have assumed that the two coupled protonation reactions – both by $(H^+)_{aq}$ – of HCO_3^- and B respectively, are diffusion-controlled. This is justified because these reactions are just the protonation reactions of moderately-strong bases (HCO_3^- and B) for a strong acid, $(H^+)_{aq}$, having formally a $pK_a = -1.74$, i.e., about 5.3 pK_a units stronger than CA. Such reactions were famously already found to be diffusion-controlled by Eigen and Weller some 60 years ago (6-9) and by many others following those authors' seminal studies.

The numerical values of the rate constants $k_{D(BC)}$ and $k_{D(HB)}$ were calculated by using equation (S3.1), with the two relative diffusion coefficients $D_{AB} = D(HCO_3^-) + D(H^+)$ and $D'_{AB} = D(B) + D(H^+)$, and the reaction radius $a = 5.5$ Å for the $(H^+)_{aq}$ protonation of HCO_3^- and B, respectively. The resulting diffusion coefficients of the reactants and the calculated rate constants $k_{D(BC)}$ and $k_{D(HB)}$ are given in Table S2. The reactants' diffusion coefficients are temperature-dependent and the temperature-dependent values are also listed in Table S1 for the two experimental temperatures. With the values of $k_{D(BC)}$ and K_a of CA, the CA dissociation reaction has a lifetime $1/k_{dis}$ in the time-range of a few hundreds of ns, making it far more unstable due to proton dissociation than due to decomposing.

The remaining two rate constants $k_{dis\,(CA)}$ and $k_{dis(HB)}$ in equation (S2.5), for the two acid overall dissociation reactions (for CA and H^+B respectively) can be related to $k_{D(BC)}$ and $k_{D(HB)}$ by the appropriate equilibrium constant relations

$$k_{dis(CA)} = k_{D(BC)}\, x10^{-pKa(CA)} \text{ and } k_{dis} = k_{D(HB)}\, x10^{-pKa(HB)} \qquad (S4.1)$$

These rate constants are listed in Table S2.

S5. Based-induced decomposition route R_{ic}. We have also included in our numerical kinetic analysis equation (9), for completeness, the possibility of a base-induced decomposition of CA, text equation (4), repeated here as reaction (S5.1), not to be confused with the spontaneous breakdown of CA to CO_2 and H_2O in aqueous solution, text equation (2).

$$H_2CO_3 + B \xrightarrow{k_{ic}} CO_2 + H_2O + B \qquad (S5.1)$$

The rate constant k_{ic} is calculated assuming that the reaction is diffusion-controlled, $k_{ic}=k_{D(B)}$; that condition represents the maximum possible effect of reaction (S5.1), i.e., the extreme reaction case where direct encounters between CA and a base do not result in CA transferring a proton to the base, but rather result in the breakdown of CA to form CO_2 and H_2O. (Even so, we found that this reaction is unimportant).

S6. Generation of kinetic plots in Fig. 3. The numerical solutions (using Matlab R 2015a program) of the four coupled rate equations (9) for the CA reactions described in text were used to fit the kinetic protonation yield data of main text Fig. 2 (see Fig. S2 below) and for simulating the 5 decay curves shown graphically for the 1N4S base in the main text Fig. 3 and for the HPTS base Fig. S3 below. Figure S2 visually shows the important feature that the full kinetic solutions of the rate equations for the CA/bicarbonate system result in an almost pure exponential decay of the protonated populations' fraction as a function of the incubation time of CA: the generated decay curves are practically identical to those shown in Fig. 2 in the main text, where the same total protonation quantum-yield data was simply fit by single exponent decay functions. The further and key point is that the exponentially fit (Fig. 2) and calculated (Fig. S2) temperature-dependent exponential decays are both practically identical to the independently determined temperature-dependent unimolecular lifetime of CA characterizing its disappearance during the incubation time due to its spontaneous breakdown to water and CO_2.

As already mentioned in the text, the analysis of text Fig. 2's experimental results in terms of determining routes of the base protonation via CA is not straightforward, due to the nature of the reactions involved and to the long-time scale of those results. If for example CA behaves kinetically more like a weak acid (as expected from its pK_a), then its overall bimolecular protonation reactions of strong bases like the ones used in our experiments would be practically by the R_d diffusion-limited route: the rate-determining step is the acid-base diffusion-controlled encounter. In the concentration range used in our experiments, this encounter would occur on a ns time scale, much shorter than the ms time-scale of our stopped flow setup. We are thus unable to directly observe in real time the PT reactions' progress. Nonetheless, important information on those reactions necessary to characterize CA's kinetic behavior can be obtained. In particular, the detailed kinetic scheme of the coupled rate equations (9) is used to predict the long-time limit of the base protonation (following rapid mixing of the base with CA) in the experiments of text Fig. 2. This was done in text Fig. 3 for the IN4S base, and for completeness, we display in Fig. S3 the corresponding results for the kinetics of the protonation of the HPTS base (of form RO^-) following rapid mixing of the base with CA as described in the main text.

The numerical solutions for the HPTS base in Fig. S3 are qualitatively and quantitatively similar to those calculated for the 1N4S base in text Fig. 3 and discussed in the main text, with the small numerical differences emerging from the differences in the reaction parameters of the two protonation reactions of the two bases. The discussion of the Fig. S3 is essentially identical to that for text Fig. 3, and is not produced here.

We have found that, in the specific conditions of our stopped-flow experiments, solution of the full kinetic system of the CA buffer has shown via text Fig. 3 and Fig. S3 that there is the

dominance of the direct R_d route over the indirect R_i protonation route. Here we provide a further discussion to provide some perspective on this dominance.

The importance of direct diffusion-limited encounter protonation route R_d equation (7) compared to that of the indirect through-water protonation R_i route equation (8) by the CA generated $(H^+)_{aq}$ depends both on the protonating acid's pK_a and the rate of acid-base encounters. This bimolecular encounter rate depends in turn on the acid and base homogeneous concentrations. Assuming a typical diffusion-limited encounter rate constant of 10^{10} $M^{-1}s^{-1}$ and concentrations of 1 mM of the acid and 10 nM of a biological base, the pseudo first-order acid-base encounter rate-constant would be 10^7 s^{-1}. In comparison, the proton dissociation rate constant of an acid [cf. equation (2)] is given (in s^{-1}) to a good approximation by $k_{diss} = 10^{10 - pKa}$, which is 10^7 s^{-1} for an acid with a $pK_a = 3$. For weaker acids, i.e., acids with $pK_a > 3$, the proton dissociation rate constant under similar conditions will be less than 10^7 s^{-1}, i.e. a slower dissociation than the acid's-encounter rate with a base, thus favoring the direct route.

The pK_a of CA is 3.5, and our experiments employ concentrations of 2 mM and 3.5 mM of CA to protonate the HPTS and 1N4S bases respectively. Thus, in our adopted experimental conditions, the direct protonation route for the reactions was anticipated to be much more important than the indirect protonation route (assuming as demonstrated in the main text in "***Testing the kinetic viability of CA as a protonating agent***" section that CA protonates like an ordinary carboxylic acid**)** as we indeed found out in the experiment**.**

S7. The one-stage stopped flow set-up and experimental procedures.

One mixing stage experiments Fig. S4. There were in effect two one mixing stage experiments common to the pK_a and lifetime determination of CA in water and for quantitatively demonstrating the protonation ability of intact CA.

We consider below the experimental determination of CA's pK_a and its temperature dependence shown in text Fig. 1. In the set-up in Fig. S3 and described in its caption, color indicators with known pK_as at the set experimental temperatures were used ─ on a time scale short comparted to CA decomposition via equation (2),see below ─ to monitor the CA acid dissociation**,** equation (3). The pK_a of CA was calculated (22-24) at each temperature by extrapolating the Henderson-Hasselbalch (HH) equation (25) equation (S7.1)

$$pK_a = pH + \log([HCO_3^-]/[H_2CO_3]) \qquad (S7.1)$$

to zero time when the initial (set) concentrations of bicarbonate anion HCO_3^- and CA still prevail before CA appreciably decomposes, providing the pK_a experimental results in text Fig. 1. Further, with the initial experimental conditions chosen so that $[HCO_3^-] = [H_2CO_3] >> [H^+]$, the HH equation gives pK_a (CA) = pH.

In addition, this one stage system was used to monitor the CA decomposition equation (2) ─ in which CA breaks down to H_2O and CO_2 ─ by following the rate at which the solution pH changed as the solution becomes less acidic due to the continuous CA concentration decrease.[22] This allowed the calculation of CA's decomposition time used in the viability of CA as a protonating agent (see Fig. 2).

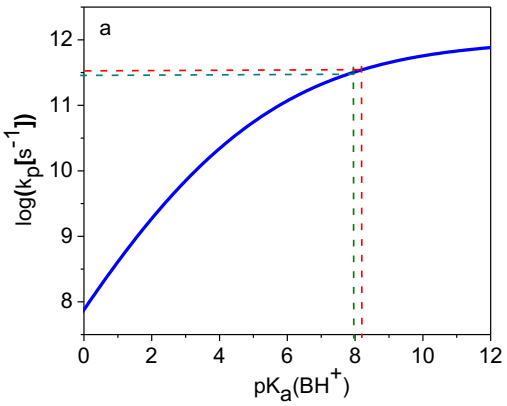

Fig. S1. **Rate constant for PT from CA to base B.** The Kiefer-Hynes on-contact rate constant for PT from of CA to B (10-13), k_p, as a function of pK_a(HB), the pK_a of the conjugate acid of the base B. The dashed lines indicate the situation for CA directly protonating 1N4S and HPTS (pK_a (H^+B = 1N4S) = 8.2 and pK_a (H^+B = HPTS) = 7.95 at zero ionic strength respectively).

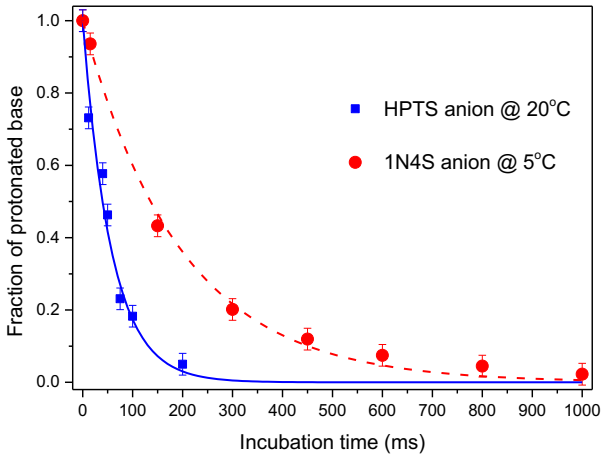

Fig. S2. Fraction of protonated bases versus Incubation time. The experimental data points were fitted by the full numerical solutions of the kinetic scheme equations (S6.1-S6.4) at a different temperature with parameters described in SI Tables S1 and S2, as opposed to the exponential fit on the Text Fig. 2. The calculated decay curves are practically identical to the exponential fits of the curves, see Fig. 2 in the main text.

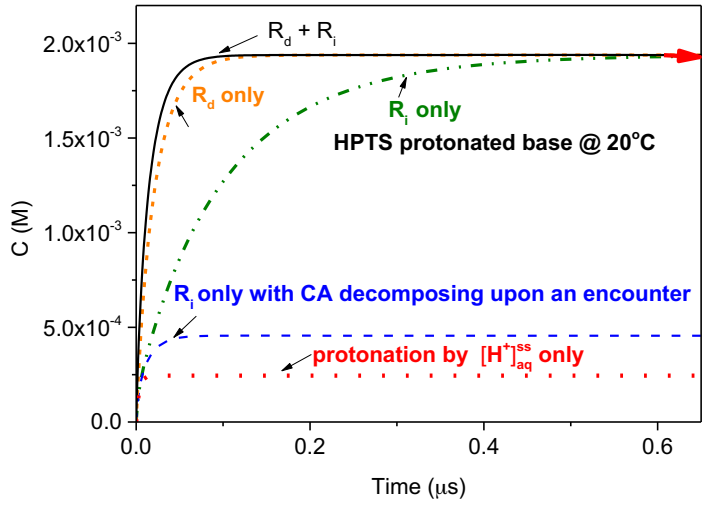

Fig. S3. Calculated kinetic profiles of the rise of the protonated HPTS base concentration. **(This is analogous to text Fig. 3 for the IN4S base).** Calculated kinetic profiles, via the numerical solution of text equations (9), of the rise of the concentration C of the protonated HPTS base ($[HPTS]_0 = 8$ mM, $pK_a(I=0) = 7.95$) absorption signal when the base is mixed in 1:1 2 mM buffer solution of H_2CO_3/HCO_3^- generated in the first mixing stage of the stopped flow experiment by mixing HCl (2mM) with sodium bicarbonate ($NaHCO_3$) 4 *mM*. Solid line: both CA's direct route R_d [equation (1)] and the indirect route R_i [equation (8)] of the base protonation are active. Dotted line: Protonation by $(H^+)_{aq}$ without participation of any CA protonation reactions. The indirect protonation via $(H^+)_{aq}$ is treated as diffusion-limited (see S4). Dashed line: now assuming that CA indirectly, but not directly, protonates the base *and* decomposes upon encountering a base molecule according to reaction equation (4). Dot-dot-dash line: assuming only the indirect protonation route R_i. Short-dash line: solution assuming only the direct protonation route R_d, but this is almost *indistinguishable* from the Solid line where both CA's direct and indirect routes R_d and R_i of the base are active. Red arrow: the stopped flow experiment's observed protonated base concentration after mixing with CA.

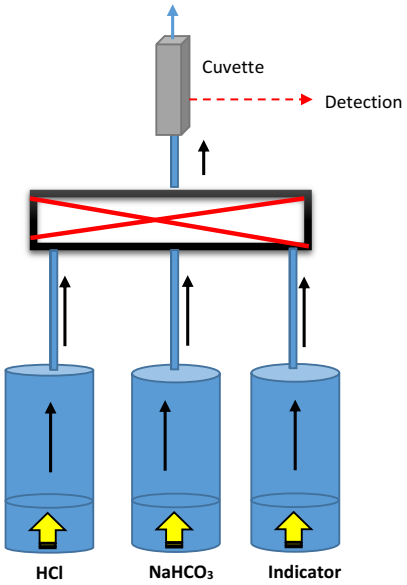

Fig. S4. A stopped-flow one-stage-mixing setup for determination of CA's $pK_a(t)$ and decomposition lifetime associated with its spontaneous decomposition to H_2O and CO_2. CA is generated by rapid acidification of bicarbonate HCO_3^- by HCl in water then reacted in the same chamber with an acid-base indicator (2,4-dinitrophenol, DNP). Temperature was controlled to within ± 0.1^0C by a variable-temperature water circulator. The concentration of the acid and base forms of the indicator were detected by absorption spectroscopy.

Table S1. Diffusion coefficients of the CA(18, 19) and base reactants(14-17) and calculated rate constants $k_{D(B)}$ and k_{off} at 20 ^{o}C and 5 ^{o}C for the direct route R_d protonations of the HPTS (20^{o}C) and 1N4S (5^{o}C) bases [cf. eqs. (S3.1) and (S3.3)].

t ^{o}C	**$D/10^{-5}$ (cm^2s^{-1})**		**$k_{D(B)}/10^9$ ($M^{-1}s^{-1}$)**	**$k_{off}/10^5$ ($M^{-1}s^{-1}$)**	
	CA	B		HPTS	1N4S
20	1.2	0.5	7.7	3.5	1.9
5	0.8	0.3	5.1	2.9	1.6

Table S2. Indirect route R_i reactant diffusion constants of HCO^-_3 (18, 19), $(H^+)_{aq}$ and base reactants (14-17) and calculated rate constants $k_{D(BC)}$ and $k_{D(HB)}$ as well as $k_{dis(CA)}$ and $k_{dis(HB)}$ for HPTS and 1N4S bases at 20°C and 5 °C.

t °C	**D/10^{-5} (cm^{2}s^{-1})**			**$k_{D(BC)}$/10^{10} (M^{-1}s^{-1})**	**$k_{D(HB)}$./10^{10} (M^{-1}s^{-1})**	**$k_{dis(CA)}$/10^7 (s^{-1})**	**$k_{dis(HB)}$/10^2 (s^{-1})**	
	HCO^-_3	B	$(H^+)_{aq}$				HPTS	1N4S
20	1.1	0.5	8.6	4.0	3.8	1.6	6.7	3.8
5	0.7	0.3	6.6	3.3	3.2	1.8	6.3	3.5

References

1. Mills GA & Urey HC (1940) The kinetics of isotopic exchange between carbon dioxide, bicarbonate ion, carbonate ion and water. *J. Am. Chem. Soc.* 62:1019-1026.
2. Roughton FJW (1941) The kinetics and rapid thermochemistry of carbonic acid. *J. Am. Chem. Soc.* 63:2930-2934.
3. Ho C & Sturtevant JM (1963) Kinetics of Hydration of Carbon Dioxide at 25 Degrees. *J. Biol. Chem.* 238(10):3499-3501.
4. Gibbons BH & Edsall. JT (1963) Rate of Hydration of Carbon Dioxide and Dehydration of Carbonic Acid at 25 Degrees. *J Biol Chem* 238:3502-3507.
5. Dewick PM (2006) *Essentials of Organic Chemistry: For Students of Pharmacy, Medicinal Chemistry and Biological Chemistry* (Wiley, Chichester, U. K.).
6. Weller A (1961) Fast reactions of excited molecules *Progr React Kinet*1:187-214.
7. Eigen M (1964) Proton Transfer, Acid-Base Catalysis, and Enzymatic Hydrolysis. Part I: Elementary Processes. *Angew Chem, Int Ed Engl* 3:1.
8. Eigen M & Hammes GG (1963) Elementary Steps In Enzyme Reactions (as Studied by Relaxation Spectrometry). in *Advances in Enzymology and Related Areas of Molecular Biology* ed Nord FF (John Wiley & Sons, Inc.), pp 1-38.
9. Eigen M, Kruse W, Maass G, & DeMaeyer L (1964) Rate constants of protolytic reactions in aqueous solution. *Prog React Kinet* 2:285.
10. Kiefer PM & Hynes JT (2002) Nonlinear Free Energy Relations for Adiabatic Proton Transfer Reactions in a Polar Environment. I. Fixed Proton Donor-acceptor Separation. *J Phys Chem A 106*:1834-1849.
11. Kiefer PM & Hynes JT (2002) Nonlinear Free Energy Relations for Adiabatic Proton Transfer Reactions in a Polar Environment. II. Inclusion of the Hydrogen Bond Vibration. *J Phys Chem A 106*:1850-1861.
12. Kiefer PM & Hynes JT (2003) Kinetic Isotope Effects for Adiabatic Proton Transfer Reactions in a Polar Environment. *J Phys Chem A 107*:9022-9039.
13. Kiefer PM & Hynes JT (2004) Adiabatic and nonadiabatic proton transfer rate constants in solution. *Solid State Ionics* 168(3-4):219-224.
14. Pines E, Magnes BZ, Lang MJ, & Fleming GR (1997) Direct Measurements of Intrinsic Proton Transfer Rates in Diffusion Controlled Reactions. *Chem Phys Lett* 281 413-420.
15. Mohammed OF, Pines D, Pines E, & Nibbering ETJ (2007) Aqueous Bimolecular Proton Transfer in Acid-base Neutralization. *Chem Phys 341*:240-257.
16. Adamczyk K, Premont-Schwarz M, Pines D, Pines E, & Nibbering ETJ (2009) Real-Time Observation of Carbonic Acid Formation in Aqueous Solution. *Science* 326(5960):1690-1694.
17. Pines D*, et al.* (2016) How Strong is Carbonic Acid? *J Phys Chem B* 120:2440−2451.
18. Li Y-H, Gregory S, & (1974) Diffusion of Ions in Sea Water and in Deep-Sea Sediments. *Geochim Cosmochim Acta* 38:703–714.
19. Zeebe RE (2011) On the Molecular Diffusion Coefficients of Dissolved CO_2, HCO_3^-, and CO_3^{2-} and Their Dependence on Isotopic Mass. *Geochim Cosmochim Acta* 75: 2483–2498.

20. Daschakraborty S*, et al.* (2016) Reaction Mechanism for Direct Proton Transfer from Carbonic Acid to a Strong Base in Aqueous Solution I: Acid and Base Coordinate and Charge Dynamics. *J Phys Chem B* 120(9):2271-2280.
21. Daschakraborty S*, et al.* (2016) Direct Proton Transfer from Carbonic Acid to a Strong Base in Aqueous Solution II: Solvent Role in Reaction Path. *J Phys Chem B* 120(9): 2281–2290.
22. Soli AL & Byrne RH (2002) CO_2 system hydration and dehydration kinetics and the equilibrium CO_2/H_2CO_3 ratio in aqueous NaCl solution. *Mar Chem* 78:65- 73.
23. Wang X, Conway W, Burns R, McCann N, & Maeder M (2010) Comprehensive Study of the Hydration and Dehydration Reactions of Carbon Dioxide in Aqueous Solution. *J Phys Chem A* 114:1734-1740.
24. Loerting T & Bernard J (2010) Aqueous Carbonic Acid (H_2CO_3). *ChemPhysChem* 11:2305 - 2309.
25. Hasselbalch KA (1917) Die Berechnung der Wasserstoffzahl des Blutes aus der freien und gebundenen Kohlensäure desselben, und die Sauerstoffbindung des Blutes als Funktion der Wasserstoffzahl. *Biochem Z* 78:112–144.